

Inventory of landslides triggered by hurricane Matthew in Guantánamo, Cuba

Yusmira Savón Vaciano

Institute of Meteorology

Ricardo Delgado Tellez

Delegation of the Ministry of Science, Technology and Environment

Enrique A. Castellanos Abella (✉ eacastellanos@gmail.com)

Ministry of Energy and Mines: Ministerio de Energia y Minas <https://orcid.org/0000-0003-2066-7681>

Rafael Guardado Lacaba

University of Moa

Arisleidys Peña de la Cruz

Institute of Meteorology

Research Article

Keywords: Landslides, Inventory, Hurricane, Matthew, Guantánamo, Cuba

Posted Date: April 12th, 2021

DOI: <https://doi.org/10.21203/rs.3.rs-333479/v1>

License: © ⓘ This work is licensed under a Creative Commons Attribution 4.0 International License. [Read Full License](#)

Abstract

An inventory of landslides triggered by Hurricane Matthew (4–5 October 2016) through the eastern region of Cuba was carried out using Sentinel 2A satellite images. The inventory was compared with the slope map generated from the digital elevation model at 25 m per pixel and with the geological map at 1: 100 000 scale. The precipitation data from the 1-hour rain gauge records of four stations of the Cuban Institute of Meteorology (INSMET) and 24-hour rain gauge records of six stations of National Institute of Hydraulic Resources (INRH) were processed and analysed during this event. In total, 237 landslides were classified into rockslides, debrisflows and topples. A wide distribution of landslides was found within the selected slope classes, depending of the landslide type. Most of the landslides were generated in green schist of volcanic and vulcanoclastic rocks and rocks of the ophiolitic complex made up of ancient remains of oceanic crust. Findings increase understanding of landslide occurrence in this area in order to update landslide hazard map and to reduce landslide risk.

Introduction

Landslide inventory databases are becoming available to more countries and several are now also available through the internet. A comprehensive landslide inventory is a must in order to be able to quantify both landslide hazard and risk (van Westen et al. 2008). A significant part of the methodologies for landslide risk assessment include as a fundamental input, detailed information on the previous occurrence of landslides in the study area (Dai et al. 2001; Ayalew and Yamagishi 2005). There have been research on landslide inventory worldwide (Brown et al. 1992), as well as nation or regional ones (Guzzetti et al. 1994; Marcelino et al. 2009).

The island of Cuba is the largest of the Caribbean region with 109 884 km² (ONEI 2020). Its eastern area is the most prone to the occurrence of landslides, due to the abundance of mountainous areas with steep slopes (Castellanos and Van Westen 2007). In Cuba, most of landslides are associated to meteorological events such as hurricanes, tropical storms or prolonged periods of rain (Castellanos and van Westen 2008). The eastern region of Cuba is frequently exposed to those meteorological phenomena due to the geographical location of the archipelago in a very active hurricane zone, according to the Chronology Report of Tropical Cyclones in Guantánamo for period 1851-2019, produced by the Guantánamo Meteorological Center. The landslide hazard, vulnerability and risk assessment carried out in Guantánamo province as part of the national effort to improve disaster management, also concluded that rainfall is the most important triggering factor for these events in the area (Savón et al. 2016).

The landslide inventory currently available for the eastern zone was carried out by photointerpretation of aerial photos from 1956 at 1:62 000 scale and 1974 at 1:37 000 scale (Castellanos and Van Westen 2008; Castellanos 2000). After these inventories, there was not an update with the occurrence of more recent significant meteorological events.

The year 2016 was a very active from the meteorological point of view for the easternmost region of Cuba due to the occurrence of events that caused heavy rainfall. In the study area there were 19 events recorded by stations of the Institute of Meteorology and the Institute of Hydraulic Resources. For a 24-hour accumulated rainfall regime, two months recorded the most heavy rain events: April with five events and accumulated rainfall of 863.3 mm; and October with 12 events of heavy rainfall and accumulated 2448.6 mm. Among these events, Hurricane Matthew stands out for its regional impact, which caused significant damage in different Caribbean islands and in the United States of America with winds corresponding to a category 3-5 hurricane on the Saffir-Simpson scale, intense rains, and coastal flooding (Ballester and Rubiera 2016; Steward 2017).

In the present work, after characterizing the rainfall of Hurricane Matthew, we presents the inventory of landslides triggered by this event as it passes through the eastern part of Cuba. The rainfall was analyzed by using rain gauge data collected by the Institute of Meteorology (INSMET) and the National Institute of Hydraulic Resources (INRH).

Study area

The area of influence of Hurricane Matthew was the eastern corner of the island of Cuba (Figure 1). Low mountains (less 600 m) predominate in this area with some frequently heights less than 1200 m, coastal plains and small intra-mountains valleys surrounded by steep slopes are the most common flat areas.

This region is complex from the lithological and structural point of view. It is composed of the rocky complexes of the Cretaceous basement, with rocks of the metamorphic complex, mainly sericite and albite schists and andesite-basaltic lavas. The layers are finely stratified and rocks of the ophiolitic complex have a high degree of fracturing. There are also rocks of the Paleogene volcanic island arc with predominance of tuffs. To a lesser degree, there are rocks of the Neogene-Quaternary coverage composed mainly by the alternation of sandstones, lutite, calcareous lutite and biotrititic limestones (Iturralde-Vinent 1998). The marine terraces composed of bioclastic and biogenic limestone, calcareous sandstone generated by a combination of recent movements of the earth's crust with the cycles of sea levels due to glaciations stand out in the coastal area (Castellanos 2000).

The mountain ranges in the area represent one of the most extensive and well-preserved mountainous ecosystems in the Antilles. Four distinct terrestrial ecoregions from the 193 recognised in the world are present: Cuban moist forest, Cuban dry forest, Cuban pine forest, and Cuban cactus scrub (Olson et al. 2001). Such diversity in a small extension rank the area among the top biodiversity hotspots in the Caribbean. The soils are highly diversified with 13 types and 18 subtypes, most of them with low crop potential mainly used for forestry.

Accordingly, there is a high concentration of fauna in this area, which is relevant for the Caribbean by its either abundance, diversity or endemism. The region is considered the oldest center of evolution of the flora of Cuba, representing one of the floristic regions with the highest endemism of the Greater Antilles, with 928 endemic species, almost 30% of those reported for Cuba, of which 366 are exclusive to the region (Borhidi 1996). There are also 22 plant formations of the 26 defined for Cuba (Puchkov et al. 1989). It is the location of the last remnants of rainforests in Cuba, considered an important productive natural ecosystem (Lastres 1988). In summary, both flora and fauna in the study area are ecologically significant for the country and the Caribbean region.

Matthew Hurricane

Tropical storm Matthew originated from a strong tropical wave, close to the southern group of the Lesser Antilles arc, in the late morning of September 28, 2016, reaching category 5 on the Saffir - Simpson scale on October 2 in the warm waters of the eastern Caribbean. It made landfall in Cuban territory on October 4 near Punta Caleta ($20^{\circ} 07' 00''$ N, $74^{\circ} 30' 10''$ W), on the south coast, at approximately 6:00 p.m. in local time, as a category 4 hurricane in the Saffir-Simpson scale. The hurricane traveled over land in the study area for 6 hours (Figure 1A), at a translation speed of 15 km/h, leaving the ground at a point near Mata Bay ($20^{\circ} 29' 30''$ N, $74^{\circ} 38' 00''$ W) on October 5 as category 3 hurricane (Ballester and Rubiera 2016).

The area of influence of the hurricane force winds extended about 84 km from the center with tropical storm force winds extended up to 154 km further as shown in Figure 1B. Hurricane Mathew has been the most intense on record for this region of Cuba. Matthew caused significant damage to agriculture, communications infrastructure, electricity and water supply services, roads, and homes in impacted communities. Economics losses were estimated at 2 430,8 million of pesos, 46 706 houses were damaged, of which 8 312 houses completely collapsed (ONEI 2017).

Figure 2 presents the accumulated rainfall of the stations during the year 2016. It is notable the significant increase in the accumulated precipitation recorded in stations 89, 1631, 78334, 712 and 1537 in October, coinciding with the occurrence of this meteorological event. Stations 89, 1631 and 78334 registered the highest accumulated in the year, they were in the order of 2309,2; 2217,3 and 1690,6 mm in the year respectively.

The highest accumulated precipitation due to Hurricane Matthew was recorded at stations 78369, 78319 and 78334 (located in Figure 1B). The day 4 was the one with the highest precipitation in the entire area affected by the meteorological event as shown in Table 1.

The rainfall associated with the hurricane and its feeding bands were intense, specifically on the days of Hurricane Matthew. It behaved as shown in Table 1, with considered raining on the day 4 in the station 78369 and on the day 5 in stations 78319 and 78334.

Table 1. Accumulated rainfall recorded the before, during and after Matthew hurricane. (*) no data.

Type	Station	Day 3	Day 4	Day 5	Day 6	Accumulated
24-hour	89	139.0	*	139.0	21.0	299.0
24-hour	712	0.0	63.4	0.0	0.0	63.4
24-hour	1537	0.0	299.0	0.0	0.0	299.0
24-hour	1538	0.0	55.8	0.0	0.0	55.8
24-hour	1594	0.0	*	*	0.0	0.0
24-hour	1631	0.0	191.0	0.0	0.0	191.0
1-hour	78356	0.8	111.0	0.0	0.0	111.8
1-hour	78319	0.0	186.1	213.9	0.1	400.0
1-hour	78334	9.0	156.2	221.5	0.7	378.4
1-hour	78369	0.0	542.0	119.0	0.0	661.0

Figure 3 shows rainfall events recorded one month before and one month after hurricane Matthews arrival. It possible to see the increasing of rainfall event with Matthews, highlighting station 78319 with 11 and 19 intensive rainfalls and the station 78334 with 12 and 16 intensive rainfalls. It is also possible to note how precipitation remains higher than before, after Hurricane Matthews crossing the Guantánamo province.

Methods

An inventory of landslides was carried out for the period from August 2016 to January 2017. The main source of information for this inventory were Sentinel 2A satellite images from MSI instrument operated by the European Space Agency (ESA). Moderate resolution (10 m per pixel) true color and false color near-infrared images were generated from level 1C products. Images dates, identifier, size and cloud percentage are shown in Table 2. The limits of the area of interest were defined taking into account the frame of topographic sheets at 1:10 000 scale. High-resolution post event satellite images provided by free internet providers Google and Microsoft where used as additional source of information.

Table 2. Satellite image data used for landslide inventory

Date/Time	Image Identifier	Cloud Percentage
2016-08-30 T15:36:22.026Z	S2A_MSIL1C_20160830T153622_N0204_R068_T18QWH_20160830T153619	36.68
2016-09-19 T15:36:12.026Z	S2A_MSIL1C_20160919T153612_N0204_R068_T18QWH_20160919T153613	6.60
2016-10-09 T15:36:12.026Z	S2A_MSIL1C_20161009T153612_N0204_R068_T18QWH_20161009T153614	40.77
2017-01-07 T15:36:01.026Z	S2A_MSIL1C_20170107T153601_N0204_R068_T18QWH_20170107T153707	9.81

The study area was divided into 183 squares of 5 x 5 km and a visual interpretation was made using the Normalized Difference Vegetation Index (NDVI), identifying the landslides. Each cell was examined and compared with the exposure of soils, rocks and the existing vegetation in it, classifying the cells taking into account the amount of landslides by squares.

After visual interpretation, field visits were made in the study area for the purpose of checking and direct identification of some landslides, as well as to confirm potential areas of occurrence of these events. Several fieldwork routes were traced through the towns affected by the hurricane.

In order to understand the behavior of the rain as a triggering factor, the precipitation data from 1-hour rain gauge stations operated by INSMET and 24-hour rain gauge stations operated by INRH for October 2016 was compiled and analyzed.

Once the landslide inventory was completed, these were spatially compared with the slope map generated from the digital elevation model at 25 m per pixel. Similarly, the inventory was compared with the geological map at 1:100 000 scale (IGP 2016).

Results And Discussion

The landslide inventory carried out in the study area found 237 events that could be associated to Hurricane Matthew taking into account the freshness of the material movement and the loss of the soil layer. Landslide were classified into three main types: rockslides, debris flows and topples. Figure 3A shows a 5 x 5 km² grid with landslide numbers by cell. As can be seen, there were areas with high occurrence of landslides that reached up to 34 counts. The vast majority were shallow landslides as shown in Figure 3B.

Regarding the relationship between the occurrence of landslides and rainfall, we found that according to the spatial location and the radius of influence of the rain gauges, most of the landslides were concentrated in the areas with the precipitation recorded by of station 78334 (see table 1 and figure 3). This finding confirms the relationship of the occurrence of landslides with events of intense rainfall found by other authors (Lumb 1975; Garland and Oliver 1993; Kay and Chen 1995; Finlay et al. 1997; Crosta 1998, 2003; Guzzetti 1998; Crozier 1999; Dai et al. 2001; Aleotti 2004; Dikshit et al. 2019; Sarkar and Dorji 2019). Station 78334 also registered intensive rains, but it is located in an area of an intra-mountain valley, which is why not many landslides occurred in that area.

Slope angle is very important as part of the conditioning factors generating landslides as mentioned by Aristazabal and Gómez (2007) and Aristizábal and Yokota (2006).

Figure 5, shows the relationship of the slope classes and elevation of the landslides in the study area. It is notable that rockslides have a wide distribution in the nine established slope angles classes, diminishing towards the 35-40° and >45° classes. Only four rockslides were found in areas with more than 45° slope angle. With respect to elevations, rockslides have their greatest distribution within the range of 100-600 m with 132 events.

In the case of topples, their distribution was limited to slopes of classes 10-15 and 15-20 with heights between 30-45 meters above sea level. These occurred in the marine terrace system as mentioned by Castellanos (2000). For the debrisflows they present their distribution within the slope classes <10°, 10-15° and 30-35°. However, in terms of elevation they are framed within 170-450 m.

Most of the rockslide-type landslides are generated in materials represented by green schists of volcanic and vulcanoclastic rocks and rocks of the ophiolitic complex constituted by ancient remains of oceanic crust and within its composition we find harzburgites, lherzolites and serpentinized dunites of the Cretaceous Lower- Upper and Middle Jurassic as shown in Table 2. These are the oldest rocks in the study area and present different degrees of weathering and high deformation.

Debris flows only occurred in rocks from the Middle Jurassic ophiolitic complex and in magmatic rocks and to a lesser degree in rocks composed of green schists of volcanic and vulcanoclastic rocks of Cretaceous age; Topples only developed in the Maya formation composed of organodetritic and organogenic limestones from the Upper Pliocene-Upper Pleistocene.

Table 2. Relation of landslide occurrence with rock types

Unit name	Rock type	Age	Landslide type		
			rockslide	debrisflow	topples
Formation La Farola	Green schists of volcanic and vulcanoclastic rocks	Lower Cretaceous-Upper Cretaceous	130	4	
Ophiolitic Complex	Rocks of the ophiolitic association: harzburgites, lherzolites, serpentinized dunites	Middle jurassic	77	6	
Magmatic rocks	Undifferentiated gabbroids, gabbros, and diabases		8	6	
Formation Guira de Jauco	Banded, granular or schisty amphibolites, partly metagabbroid, with intercalations of gneisses and metasilicites	Jurassic-Lower Cretaceous	1		
Member Cilindro	Polymictic conglomerates with lenticular stratification and sometimes crossed, weakly cemented, with sandstone lenses, containing lignite. The matrix is polymictic sandstone, containing carbonate.	Upper Oligocene-Lower basal Miocene	2		
Formation Jaimainita	Massive biotrititic limestones, generally karst, very fossiliferous.	Upper Pleistocene.			1
Formation Maya	Marine Deposits, Organodetritic and Organogenic Limestones.	Upper Pliocene-Upper Pleistocene			2

Conclusions

Hurricane Mathew affected Guantánamo province in Eastern Cuba triggering 237 landslides as interpreted by satellite images. The majority of the landslides found were rockslides with a small amount of debrisflows and topples. The areas with higher rainfall coincides with highest landslides occurrence, except for intra mountain valleys, which is in accordance with the nature of the event.

Slope angle does not seem to represent a factor as important as the rock type in the area, since many landslides occurred in slopes lower than 45°. Most of landslides were located in green schists of volcanic and vulcanoclastic rocks, as well as rocks of the ophiolitic association: harzburgites, lherzolites and serpentized dunites.

This landslide inventory contributes to previous efforts in reducing landslide risk in the mountain areas of Guantánamo province and are the base to updating landslide susceptibility and hazard maps in the region.

Declarations

Funding: This research was supported by the Institute of Meteorology of Cuba.

Conflicts of interest/Competing interests: Information provided in this manuscript does not have any conflict or competing of interests.

Availability of data and material: Authors confirm that data provided in this research is available at the Meteorological Center in Guantánamo province in Cuba.

Code availability: No applicable.

Authors' contributions: No applicable.

Ethics approval: No applicable.

Consent to participate: All authors consent to participate in this research.

Consent for publication: All authors consent to participate in this publication.

References

Aleotti P (2004) A warning system for rainfall-induced shallow failures. *Eng. Geol.* 73:247–265.
<https://doi.org/10.1016/j.enggeo.2004.01.007>

Aristizábal E, Gómez J (2007) Inventario de emergencias y desastres en el valle de aburrá. originados por fenómenos naturales y antrópicos en el periodo 1880-2007. *Gestión y Ambiente* 10(2):17-30.
<https://revistas.unal.edu.co/index.php/gestion/article/view/1409>

Aristizábal E, Yokota S (2006) Geomorfología aplicada a la ocurrencia de deslizamientos en el valle de aburra. *DYNA* 73(149):05-16. <https://revistas.unal.edu.co/index.php/dyna/article/view/807>

Ayalew L, Yamagishi H (2005) The application of GISbased logistic regression for landslide susceptibility mapping in the Kakuda-Yahiko Mountains, Central Japan. *Geomorphology* 65:15–31.
<https://doi.org/10.1016/j.geomorph.2004.06.010>

Ballester M, Rubiera J (2016) Summary of cyclone season 2016 in North Atlantic, Institute of Meteorology (INSMET), Ministry of Science, Technology and Environment, Cuba. <http://www.insmet.cu/asp/genesis.asp?TB0=PLANTILLAS&TB1=TEMPORADA&TB2=/Temporadas/temporada2016.html#home>

Borhidi A (1996) *Phytogeography and Vegetation Ecology of Cuba*. Akademiai Kiadó, Budapest.

Brown WM, Cruden DM, Denison JS (1992) The directory of the world landslide inventory. USGS Open File Report 92-427-A, 239 p.

- Castellanos Abella, E.A. (2000) Design of a GIS-Based System for Landslide Hazard Management, San Antonio del Sur, Cuba, case study. M.Sc. Thesis, International Institute for Aerospace Survey and Earth Sciences (ITC), Enschede, 108 pp.
- Castellanos EA, Van Westen CJ (2007) Generation of a landslide risk index map for Cuba using spatial multi-criteria evaluation. *Landslides* 4: 311–325. <https://doi.org/10.1007/s10346-007-0087-y>
- Castellanos EA, Van Westen CJ (2008) Qualitative landslide susceptibility assessment by multicriteria analysis: A case study from San Antonio del Sur, Guantánamo, Cuba. *Geomorphology* 94(3-4):453-466.
<https://doi.org/10.1016/j.geomorph.2006.10.038>
- Crosta GB (1998) Regionalization of rainfall thresholds: an aid to landslide hazard evaluation. *Environ. Geol.* 35:131–145.
<https://doi.org/10.1007/s002540050300>
- Crosta GB (2003) Distributed modelling of shallow landslides triggered by intense rainfall. *Nat. Hazard Earth Syst. Sci.* 3:81–93. [hal-00299004](https://doi.org/10.1007/s002540000163)
- Crozier MJ (1999) Prediction of rainfall-triggered landslide: a test of antecedent water status model. *Earth Surf. Process. Landf.* 24:825–833. [https://doi.org/10.1002/\(SICI\)1096-9837\(199908\)24:9<825::AID-ESP14>3.0.CO;2-M](https://doi.org/10.1002/(SICI)1096-9837(199908)24:9<825::AID-ESP14>3.0.CO;2-M)
- Dai F, Lee C, Li J et al (2001) Assessment of landslide susceptibility on the natural terrain of Lantau Island, Hong Kong. *Environ. Geol.* 40:381–391. <https://doi.org/10.1007/s002540000163>
- Dikshit A, Sarkar R, Pradhan B et al (2019) Estimating Rainfall Thresholds for Landslide Occurrence in the Bhutan Himalayas. *Water* 11. <https://doi.org/10.3390/w11081616>
- Finlay PJ, Fell R, Maguire PK (1997) The relationship between the probability of landslide occurrence and rainfall. *Can. Geotech. J.* 36:811–824. <https://doi.org/10.1139/t97-047>
- Garland GG, Oliver MJ (1993) Predicting landslides from rainfall in a humid, sub-tropical region. *Geomorphology* 8:165–173. [https://doi.org/10.1016/0169-555X\(93\)90035-Z](https://doi.org/10.1016/0169-555X(93)90035-Z)
- Guzzetti F (1998) Hydrological triggers of diffused landsliding. *Environ. Geol.* 35:2–3.
- Guzzetti F, Cardinalli M, Reichenbach P (1994) The AVI project: a bibliographical and archive inventory of landslides and floods in Italy. *Environ. Manage.* 18:623-633 <https://doi.org/10.1007/BF02400865>
- IGP, 2016. Mapa Geológico de Cuba a escala 1:100 000. Instituto de Geología y Paleontología, 120 pp.
- Iturralde-Vinent MA (1998) Sinopsis de la Constitución Geológica de Cuba». *Acta geológica hispánica* 33:9-56.
<https://www.raco.cat/index.php/ActaGeologica/article/view/75545>
- Kay JN, Chen T (1995) Rainfall-landslide relationship for Hong Kong. *Proceeding ICE. Geotechnical Engineering* 113:117–118. <https://doi.org/10.1680/igeng.1995.27592>
- Lastres, O., 1988. Dynamics of organic and energy reserves of litter in a semi-deciduous tropical forest in Cuba, PhD Thesis. University of Eastern, Santiago de Cuba, Cuba.
- Lumb P (1975) Slope failure in Hong Kong. *Q. J. Eng Geol. Hydrogeol.* 8:31–65.
<https://doi.org/10.1144/GSL.QJEG.1975.008.01.02>
- Marcelino EV, Fromaggio AR, Maeda EE (2009) Landslide inventory using image fusion techniques in Brazil, *Int. J. Appl. Earth Obs. Geoinf.* 11:181-191. <https://doi.org/10.1016/j.jag.2009.01.003>

Olson DM, Dinerstein E et al (2001) Terrestrial Ecoregions of the World: A New Map of Life on Earth: A new global map of terrestrial ecoregions provides an innovative tool for conserving biodiversity. *BioScience* 51:933–938.

[https://doi.org/10.1641/0006-3568\(2001\)051\[0933:TEOTWA\]2.0.CO;2](https://doi.org/10.1641/0006-3568(2001)051[0933:TEOTWA]2.0.CO;2)

ONEI (2017) Anuario Estadístico de Cuba 2016, Medio Ambiente, Oficina Nacional de Estadísticas e Información (ONEI), 59 pp.

ONEI (2020) Anuario Estadístico de Cuba 2019, Territorio, Oficina Nacional de Estadísticas e Información (ONEI), 14 p.

Puchkov AI, Marrero A, Fariñas A, Fernandez A, Salaur A, Campos AA, Florido A (1989) Nuevo Atlas Nacional de Cuba. La Habana. <https://www.ign.es/web/catalogo-cartoteca/resources/html/023661.html>. Accessed 31 January 2021

Sarkar R, Dorji K (2019) Determination of the Probabilities of Landslide Events—A Case Study of Bhutan. *Hidrology* 6. <https://doi.org/10.3390/hydrology6020052>

Savón Y, Mesa AM et al 2016. Evaluación del peligro de ocurrencia de movimientos gravitacionales en la provincia Guantánamo. *Revista Hombre ciencia y Tecnología* 20(3):112-121.

<http://www.ciencia.gtmo.inf.cu/index.php/http/article/view/747>

Stewart SR (2017) Hurricane Matthew. AL142016. 28 September - 9 October. National Hurricane Center. Tropical Cyclone Report, 96 p.

Van Westen CJ, Castellanos EA, Kuriakose SL (2008) Spatial data for landslide susceptibility, hazard and vulnerability assessment: an overview. *Eng. Geol.* 102(3-4):112-131.

<https://www.sciencedirect.com/science/article/abs/pii/S0013795208001786>

Figures

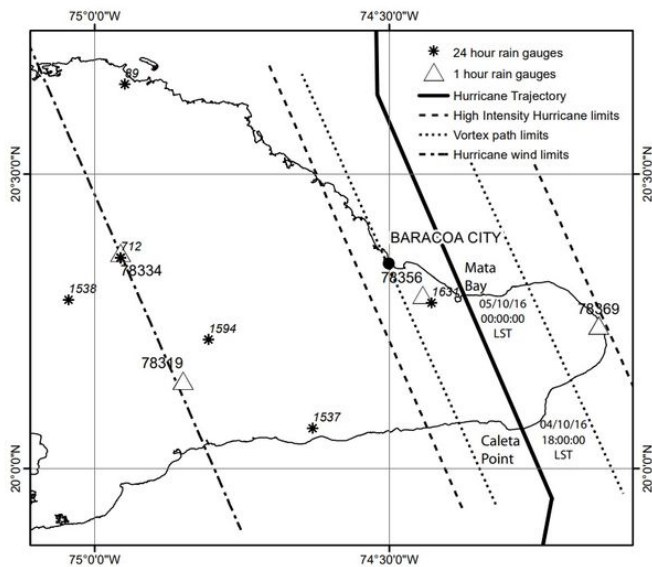
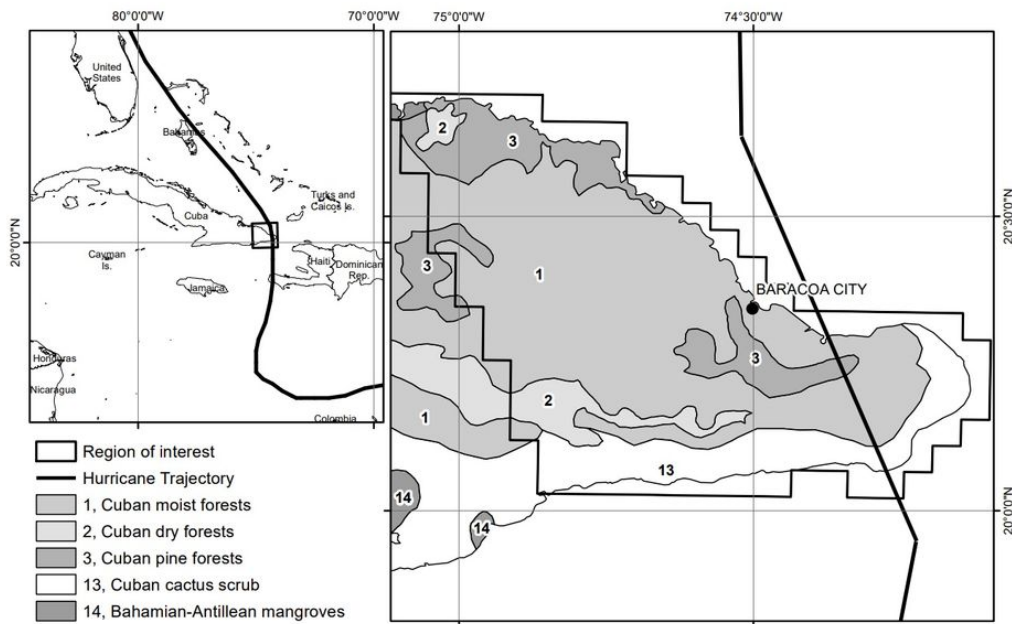


Figure 1

a) Location of Study Area, hurricane Matthew track and regions of ecological interest (after Olson et. Al 2001). b) Affected zone of hurricane Matthew and rain gauge location (after Ballester and Rubiera, 2016; and Steward 2017)

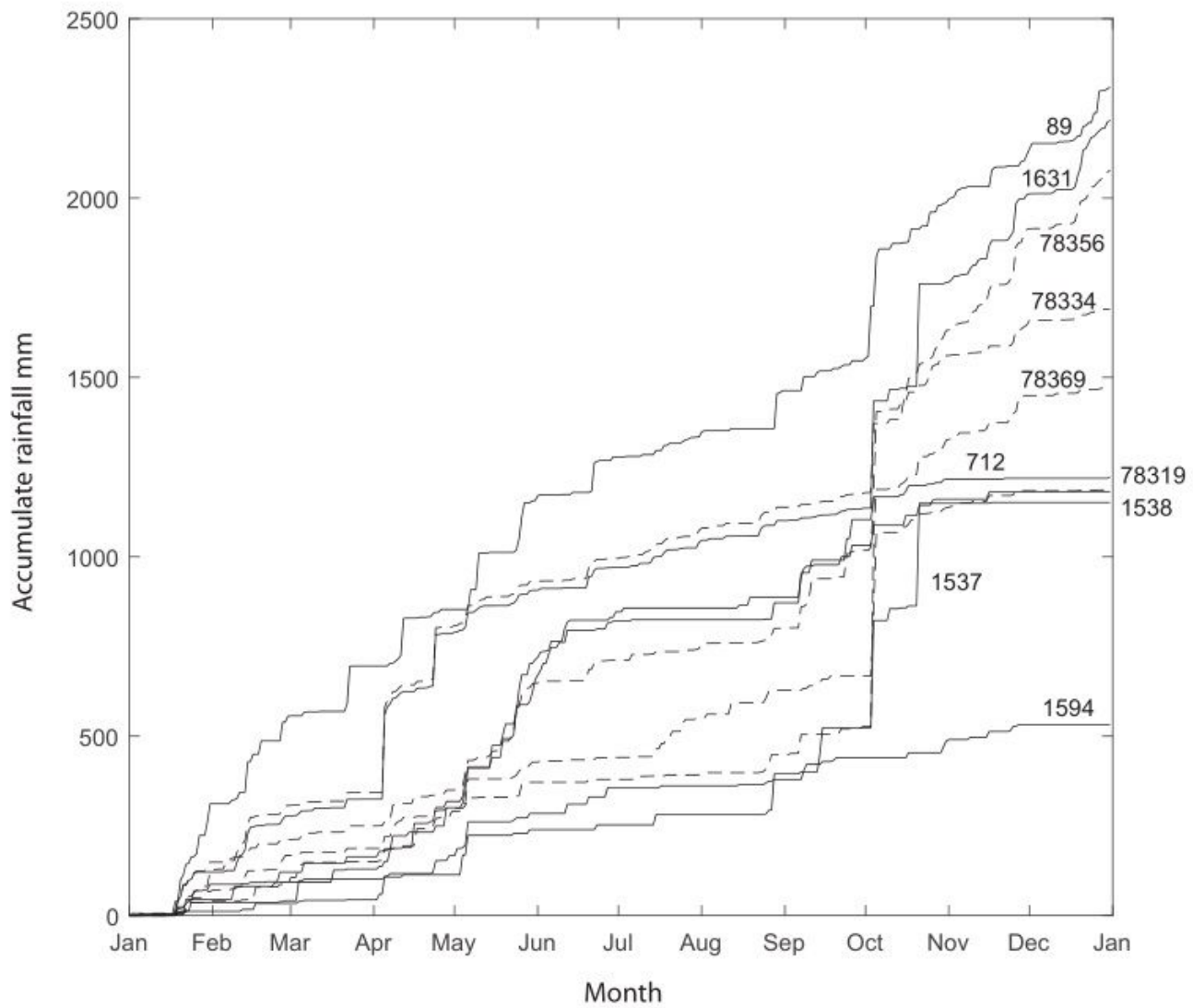


Figure 2

Accumulated rainfall recorded by the 1-hour (dashed line) and 24-hour (straight line) rain gauge stations in 2016

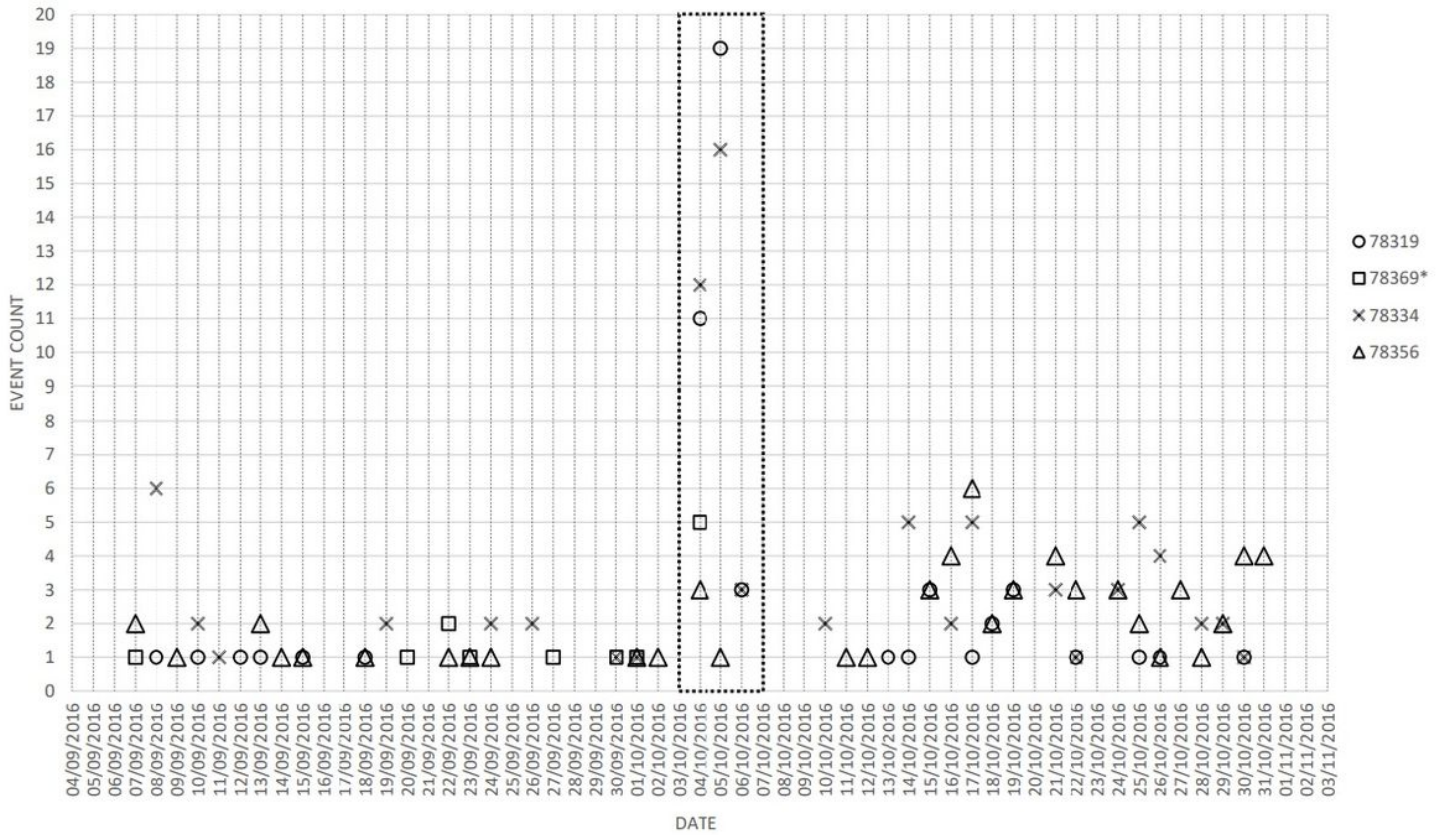


Figure 3

Rainfall events recorded in the study area for 1-hour rain gauge stations. *The gauge station 78369 suffered a catastrophic failure at 04/10/2016-21:00:00 due the effects of the hurricane force winds and was unable to record data after that point

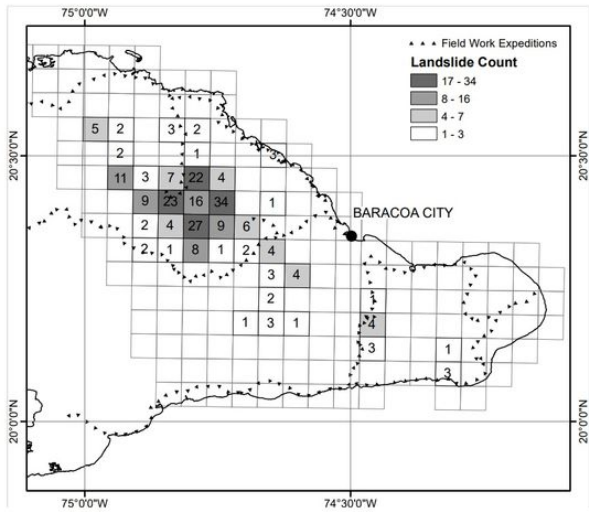


Figure 4

Landslides triggered by hurricane Matthew. a) Landslides counting in grids 5 x 5 km², rain gauge stations and fieldwork routes are included. b) Landslide photos taken on 27.11.2016

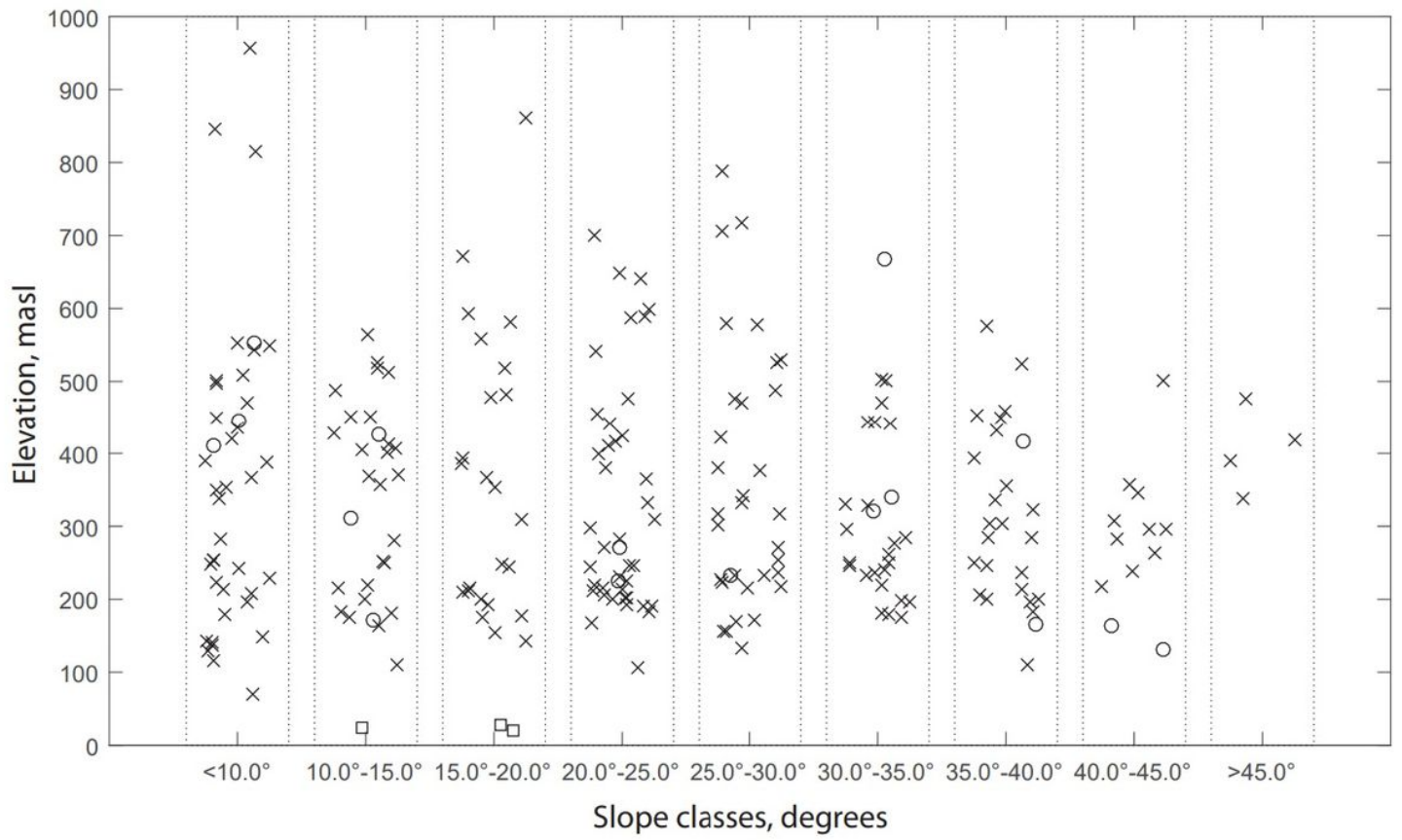


Figure 5

Landslides types compared with elevation and slope classes. Circles: debris flows, crosses: rockslides and squares: topples